

symmetric ring-breathing mode should split into four components ( $a_g + b_g + a_u + b_u$ ) under  $C_{2h}$  unit cell symmetry, the g and u modes being Raman and IR active, respectively. This splitting was not observed at ambient pressure, however, indicating that the intermolecular coupling between the molecules in the unit cell is weak but may be increased by applying pressure, eventually resulting in the observed peak broadening. The origin of the coupling may arise from the ring-ring interaction, which has been calculated to be the largest contributor to the intermolecular interaction at ambient pressure.<sup>6</sup> Very recently, Coffey and co-workers<sup>19</sup> have examined the high-pressure IR spectra of a series of  $C_2$  hydrocarbon ligands coordinated to a triosmium framework and found that the values of  $d\nu/dP$  follow the order: C-H stretching > C-C stretching > C-H bending. In our study of  $CpRe(CO)_3$ , no such conclusion could be drawn owing to the complex spectrum of the Cp ligand.

The pressure dependence of the ring tilt at  $349\text{ cm}^{-1}$  is twice that of the antisymmetric ring tilt in ferrocene.<sup>17</sup> High-pressure IR studies of some metal-sandwich compounds by Nakamoto and co-workers<sup>20</sup> have indicated that the metal-ring stretching vibration is more pressure sensitive than is the ring tilt vibration. However, these two vibrations have almost same  $d\nu/dP$  value in  $CpRe(CO)_3$ .

All values of the relative pressure sensitivity,  $d \ln \nu/dP$ , are typical of those found for internal vibrational modes except for

three bands initially at  $129\text{ cm}^{-1}$  (Cp-Re-(CO)<sub>3</sub> bending (e)),  $114\text{ cm}^{-1}$  (C-Re-C bending (e)), and  $100\text{ cm}^{-1}$  (C-Re-C bending (a<sub>1</sub>)). These three internal modes shift with increasing pressure at rates much faster than normal. The large  $d \ln \nu/dP$  value of some low-frequency internal modes may result from the coupling with external modes. However, according to Chhor and Lucazeau,<sup>10</sup> this does not occur for  $CpRe(CO)_3$ . The C-Re-C bending vibrations are expected to be less sensitive than the corresponding stretching vibrations because they are less affected by the volume change of crystal. But the reverse is observed in our work. It is possible that the larger  $d \ln \nu/dP$  values for the C-Re-C bending modes may result from slight changes in the C-Re-C angles upon application of pressure from its average value of  $90^\circ$ ,<sup>8</sup> because a pressure-induced angle change will certainly increase the restoring potential and at the same time the energy of the bending mode. As pointed out by Elian and co-workers,<sup>21</sup> the (O)C-M-C(O) angle in such a system is extremely sensitive to the extent of mixing between the carbonyl molecular orbitals and to the nature of the other ligands present. If it is again considered that pressure facilitates electron density transfer from the Cp ring to the Re metal, then the C-Re-C angle should become larger with increasing pressure.

**Acknowledgment.** This research work was generously supported by grants from the NSERC and CANMET (Canada) and the FCAR (Quebec). Y.H. acknowledges the award of a graduate fellowship from McGill University.

- (19) Coffey, J. L.; Drickamer, H. G.; Park, J. T.; Roginski, R. T.; Shapley, J. R. *J. Phys. Chem.* **1990**, *94*, 1981.  
 (20) Nakamoto, K.; Udovich, C.; Ferraro, J. R.; Quattrocchi, A. *Appl. Spectrosc.* **1970**, *24*, 606.

- (21) Elian, M.; Chen, M. M. L.; Mingos, D. M. P.; Hoffmann, R. *Inorg. Chem.* **1976**, *15*, 1148.

Contribution from the Institut für Anorganische Chemie der Universität, Auf der Morgenstelle 18, D-7400 Tübingen 1, West Germany

## Phosphorus-31 Solid-State NMR Studies of Cyclic and Acyclic Phosphine-Metal Complexes. Determination of Chemical Shift Anisotropy, Scalar Coupling $^1J_{M-P}$ (M = $^{55}\text{Mn}$ , $^{95/97}\text{Mo}$ , $^{183}\text{W}$ ), and $^{55}\text{Mn}$ Quadrupolar Coupling Constants

Ekkehard Lindner,\* Riad Fawzi, Hermann August Mayer, Klaus Eichele, and Klaus Pohmer

Received June 28, 1990

The  $^{31}\text{P}$  chemical shift tensors of cyclic and acyclic metal phosphine complexes of the type  $[M]PPh_2R$  ( $[M] = (\text{OC})_4\text{BrMn}$  (1),  $\text{Cp}(\text{OC})_2\text{ClW}$  (2),  $\text{Cp}(\text{OC})_2\text{MeW}$  (3); R = Et (a), Pr (b), Bu (c), Pe = Pentyl (d)) and  $[M]PPh_2(\text{CH}_2)_n$  ( $[M] = (\text{OC})_4\text{Mn}$  (4),  $\text{Cp}(\text{OC})_2\text{W}$  (5),  $\text{Cp}(\text{OC})_2\text{Mo}$  (6);  $n = 3$  (b), 4 (c));  $[M] = (\text{OC})_4\text{MnSO}_2$  (7);  $n = 2$  (b), 3 (c), 4 (d)) are determined by solid-state NMR techniques and correlated to structural features of the compounds. In general the isotropic chemical shift in the solid-state was found to be of the same order as the chemical shift in solution. There are differences in the tensor components due to structural changes for the manganese complexes 1. Different bond weakening abilities of a ligand (trans influence) in complexes 2 and 3 cause a large change of only one tensor component, while the other components remain constant. A "crossover" of the center shielding tensor component and the low-field component is observed for the five- and six-membered rings 4b-7b and 4c-7c, respectively.  $^{55}\text{Mn}$ - and  $^{95/97}\text{Mo}$ - $^{31}\text{P}$  coupling constants have been observed that are not obtainable in solution. The different spacings within the multiplets of the  $^{31}\text{P}$  CP/MAS spectrum of the manganese complex 1d allows us to estimate the quadrupolar coupling constant  $\chi$  and the asymmetry parameter  $\eta$  of the electric field gradient at manganese.

### Introduction

Today high-resolution  $^{31}\text{P}$  NMR spectroscopy in solution is a widely used method with manifold applications in the observation of changes in bonding and stereochemistry of phosphorus compounds.<sup>1</sup> In these studies the diagnostic manner in which the spectra reflect the local environments of the nuclei is a key feature. Generally, a correlation of spectral information to structural details is difficult. Within a series of mutually related compounds, the problems are reduced in a first approximation to one structural parameter as the major contributor that determines the spectrum. In this way it is possible to correlate  $\delta(^{31}\text{P})$  empirically with various

parameters. Examples are the definition of group contributions to the chemical shift of phosphines,<sup>2</sup> the coordination shift  $\Delta\delta$  on complexation of phosphines to metal fragments,<sup>3</sup> the dependence of  $\delta(^{31}\text{P})$  in complexes on the cone angle of the ligand,<sup>4</sup> and the ring contribution  $\Delta_R$  for phosphorus atoms involved in chelate rings.<sup>5</sup>

The last effect, in particular, has been well-known since one of the first publications about  $^{31}\text{P}$  NMR studies on organometallic compounds.<sup>6</sup> Later investigations showed a clear dependence of

(1) *Phosphorus-31 NMR Spectroscopy in Stereochemical Analysis: Organic Compounds and Metal Complexes*; Verkade, J. G., Quin, L. D., Eds.; VCH Publishers: Deerfield Beach, FL, 1987.

(2) Grim, S. O.; McFarlane, W.; Davidoff, E. F. *J. Org. Chem.* **1967**, *32*, 781.  
 (3) Mann, B. E.; Masters, C.; Shaw, B. L.; Slade, R. M.; Stainbank, R. E. *Inorg. Nucl. Chem. Lett.* **1971**, *7*, 881.  
 (4) Tolman, C. A. *Chem. Rev.* **1977**, *77*, 313.  
 (5) Garrou, P. E. *Chem. Rev.* **1981**, *81*, 229.

**Table I.** Solid-State and Solution <sup>31</sup>P NMR Isotropic Chemical Shifts (ppm)<sup>a</sup> and Coupling Constants (Hz) of Compounds 1–7<sup>b</sup>

compd	no.	δ <sub>iso</sub> (solid)	<sup>1</sup> J <sub>M-P</sub> (solid)	d <sup>c</sup>	δ(soln)	<sup>1</sup> J <sub>M-P</sub> (soln)	δ <sub>iso</sub> (solid) – δ(soln)
(OC) <sub>4</sub> BrMnPPh <sub>2</sub> Et	1a	42.4	197 (9)	44 (9)	38.7		3.7
(OC) <sub>4</sub> BrMnPPh <sub>2</sub> Pr	1b	36.2	207 (5)	41 (9)	35.8		0.8
(OC) <sub>4</sub> BrMnPPh <sub>2</sub> Bu	1c	35.9	203 (9)	36 (14)	37.0		-1.1
(OC) <sub>4</sub> BrMnPPh <sub>2</sub> Pe	1d	38.9	210 (3)	41 (4)	36.8		2.1
<i>cis</i> -Cp(OC) <sub>2</sub> ClWPPh <sub>2</sub> Bu	2c	13.3	259 (9)		12.7	264.4	0.6
<i>trans</i> -Cp(OC) <sub>2</sub> MeWPPh <sub>2</sub> Et	3a	33.8	236 (6)		30.3	247.8	3.5
<i>trans</i> -Cp(OC) <sub>2</sub> MeWPPh <sub>2</sub> Pr	3b	30.8	231 (11)		26.6	247.4	4.2
<i>trans</i> -Cp(OC) <sub>2</sub> MeWPPh <sub>2</sub> Bu	3c	29.2			27.0	247.8	2.2
<i>trans</i> -Cp(OC) <sub>2</sub> MeWPPh <sub>2</sub> Pe	3d	26.1			27.0	247.8	-0.9
		28.5	246 (14)		27.0	247.8	1.5
(OC) <sub>4</sub> MnPPh <sub>2</sub> (CH <sub>2</sub> ) <sub>3</sub>	4b	84.2			82.2		2.0
(OC) <sub>4</sub> MnPPh <sub>2</sub> (CH <sub>2</sub> ) <sub>4</sub>	4c	41.4			43.2		-1.8
Cp(OC) <sub>2</sub> WPPh <sub>2</sub> (CH <sub>2</sub> ) <sub>3</sub>	5b	74.0	290 (4)		64.9	311.0	9.1
Cp(OC) <sub>2</sub> WPPh <sub>2</sub> (CH <sub>2</sub> ) <sub>4</sub>	5c	16.4	285 (8)		11.6	285.3	4.8
Cp(OC) <sub>2</sub> MoPPh <sub>2</sub> (CH <sub>2</sub> ) <sub>3</sub>	6b	100.3	190 (38)		91.8		8.5
Cp(OC) <sub>2</sub> MoPPh <sub>2</sub> (CH <sub>2</sub> ) <sub>4</sub>	6c	51.3	159 (7)		47.3		4.0
(OC) <sub>4</sub> MnPPh <sub>2</sub> (CH <sub>2</sub> ) <sub>2</sub> SO <sub>2</sub>	7b	72.0	214 (3)	-12 (4)	72.6		-0.6
(OC) <sub>4</sub> MnPPh <sub>2</sub> (CH <sub>2</sub> ) <sub>3</sub> SO <sub>2</sub>	7c	24.4	206 (1)	-5 (1)	28.8		-4.4
(OC) <sub>4</sub> MnPPh <sub>2</sub> (CH <sub>2</sub> ) <sub>4</sub> SO <sub>2</sub>	7d	50.5	209 (2)	-1 (2)	45.8		4.7

<sup>a</sup> Relative to external 85% H<sub>3</sub>PO<sub>4</sub>. <sup>b</sup> Abbreviations: Me = methyl, Et = ethyl, Pr = propyl, Bu = butyl, Pe = pentyl, Ph = phenyl, Cp = η<sup>5</sup>-cyclopentadienyl. <sup>c</sup> Cf. eq. 1.

δ(<sup>31</sup>P) on the ring size. Compared to the signals of corresponding acyclic compounds,<sup>5</sup> the signal of the phosphorus in five-membered metallacycles is shifted 20–50 ppm to lower field while the phosphorus signal in six-membered rings resonates 2–17 ppm at higher fields. In an earlier paper considering this ring effect on the phosphorus-31 shielding, we compared the isotropic chemical shifts in the solid state with structural data derived from single-crystal X-ray diffraction experiments on cyclic and acyclic phosphine complexes of manganese and tungsten.<sup>7</sup> We were able to show that the acyclic compounds and the six-membered cycles have staggered conformations and similar chemical shifts. The five-membered cycles have eclipsed conformations and were found to be downfield-shifted compared to their homologues.

In the solid state, a nucleus undergoes a variety of observable interactions with its environment that often have a characteristic influence on its NMR spectrum. The magnitudes of these influences are strongly dependent on the orientation of the interaction relative to the external magnetic field and are best described as 3 × 3 matrices.<sup>8</sup> In solution, the isotropic tumbling of molecules reduces the interactions to the trace of the matrix, which results in the isotropic value. In the case of dipolar and quadrupolar coupling, the trace becomes zero, leaving the resonance unaffected. However, in the solid state, no such isotropic motion exists; thus a shift, broadening, and/or splitting of the resonances is caused by chemical shift anisotropy and dipolar and quadrupolar interactions. These interactions provide additional structural information that may be extracted from a solid-state NMR spectrum.

In the present paper, we wish to report how chemical shift anisotropy (CSA) and quadrupolar coupling influence the solid-state <sup>31</sup>P NMR spectra of cyclic and acyclic phosphine–metal complexes and discuss these effects in terms of the geometry of the complexes or the properties of the ligands.

**Experimental Section**

**A. NMR Spectroscopy.** Cross-polarization<sup>8</sup> magic-angle-spinning <sup>31</sup>P CP/MAS NMR spectra were obtained on a Bruker MSL-200 wide-bore spectrometer operating at 4.7 T (<sup>31</sup>P at 81.000 MHz) in a double-bearing Bruker <sup>31</sup>P CP/MAS probe and using a sweep width up to 62 kHz, a recycle time of 2 s, and a contact time of 5 ms. The isotropic lines were identified via experiments at different spinning rates. Reported tensor

components are mean values obtained from different measurements at spinning rates between 1.0 and 3.7 kHz. Numbers for these measurements are given in the last column of Table II. The standard deviations denote the scattering of these measurements. An absolute error of 5 ppm is estimated; that for the manganese complexes is 10 ppm. Between 200- and 300-mg samples of compound were spun in ZrO<sub>2</sub> rotors. Chemical shifts were referenced to an external sample of 85% H<sub>3</sub>PO<sub>4</sub>. The solution <sup>31</sup>P{<sup>1</sup>H} NMR spectra were recorded at 32.392 MHz on a Bruker WP-80 spectrometer at 243 K; chemical shifts were referenced to external 85% H<sub>3</sub>PO<sub>4</sub> in acetone-*d*<sub>6</sub>. The high-frequency–positive convention has been used in reporting all chemical shifts.

**B. Synthesis.** Compounds 1, 2, 3a–c, 4, 5, 7, 6b,<sup>9</sup> and 7<sup>10</sup> were prepared as previously described. Compounds 3d and 6c were prepared in an analogous manner.<sup>7</sup>

*trans*-Cp(OC)<sub>2</sub>MeWPPh<sub>2</sub>Pe (3d): yellow solid; yield 54%; mp 88 °C; IR (ν<sub>CO</sub> in CHCl<sub>3</sub>) 1923 s, 1831 vs cm<sup>-1</sup>. Anal. Calcd for C<sub>25</sub>H<sub>29</sub>O<sub>2</sub>PW: C, 52.10; H, 5.07. Found: C, 51.79; H 4.98.

Cp(OC)<sub>2</sub>MoPPh<sub>2</sub>(CH<sub>2</sub>)<sub>4</sub> (6c): yellow solid; yield 42%; mp 178 °C; IR (ν<sub>CO</sub> in CHCl<sub>3</sub>) 1929 vs, 1845 s cm<sup>-1</sup>. Anal. Calcd for C<sub>23</sub>H<sub>23</sub>O<sub>2</sub>MoP: C, 60.27; H, 5.06. Found: C, 61.01; H, 5.34.

**Results and Discussion**

As a manifestation of the three-dimensional nature of the chemical shielding, the spectrum of a stationary powdered sample will show a chemical shift anisotropy (CSA) pattern.<sup>8</sup> The singularities in this powder pattern correspond to the principal elements of the chemical shift tensor (Figure 1a). Magic-angle spinning (MAS) at rotating speeds much below the powder line width causes the patterns to break up into a sharp isotropic line δ<sub>iso</sub>(solid) = (δ<sub>11</sub> + δ<sub>22</sub> + δ<sub>33</sub>)/3, flanked by spinning sidebands (Figure 1b,c).<sup>11</sup> The intensities of the spinning sidebands are related to the CSA and provide an opportunity to recover the chemical shift parameters by graphical analysis.<sup>12</sup>

The isotropic chemical shifts obtained from the <sup>31</sup>P NMR spectra of complexes 1–7 in solution and in the solid state show no significant deviations (Table I), which indicates that there are no substantial structural changes between the solid state and the solution. Exceptions are 5b and 6b, due to different ring conformations in solution and in the solid state, which was established by <sup>1</sup>H (400 MHz) NMR spectroscopy in solution and single-crystal X-ray diffraction in the solid state.<sup>7</sup>

(6) Meriwether, L. S.; Leto, J. R. *J. Am. Chem. Soc.* **1961**, *83*, 3192.  
 (7) Lindner, E.; Fawzi, R.; Mayer, H. A.; Eichele, K.; Pohmer, K. *J. Organomet. Chem.* **1990**, *386*, 63.  
 (8) Mehring, M. In *High Resolution NMR Spectroscopy in Solids*; Diehl, P., Fluck, E., Eds.; NMR Basic Principles and Progress 11; Springer Verlag: Berlin, 1976.

(9) Lindner, E.; Küster, E. U.; Hiller, W.; Fawzi, R. *Chem. Ber.* **1984**, *117*, 127.  
 (10) Lindner, E.; Funk, G. *J. Organomet. Chem.* **1981**, *216*, 393.  
 (11) Maricq, M. M.; Waugh, J. S. *J. Chem. Phys.* **1979**, *70*, 3300.  
 (12) Herzfeld, J.; Berger, A. E. *J. Chem. Phys.* **1980**, *73*, 6021.

**Table II.** Calculated  $^{31}\text{P}$  NMR Chemical Shift Anisotropy Parameters<sup>a</sup> for Compounds 1–7<sup>b</sup>

compd	no.	$\delta_{11}$	$\delta_{22}$	$\delta_{33}$	$\mu^c$	$\Delta\delta^d$	$\rho, \%$	no. of spinning rates
(OC) <sub>4</sub> BrMnPPh <sub>2</sub> Et	1a	86 (0)	55 (2)	-16 (2)	102	67	39	2
(OC) <sub>4</sub> BrMnPPh <sub>2</sub> Pr	1b	87 (0)	44 (3)	-23 (3)	110	77	22	2
(OC) <sub>4</sub> BrMnPPh <sub>2</sub> Bu	1c	91 (7)	47 (10)	-32 (3)	123	84	28	2
(OC) <sub>4</sub> BrMnPPh <sub>2</sub> Pe	1d	94 (1)	41 (1)	-20 (0)	114	84	7	2
cis-Cp(OC) <sub>2</sub> ClWPPh <sub>2</sub> Bu	2c	51 (2)	16 (1)	-28 (1)	79	57	11	4
trans-Cp(OC) <sub>2</sub> MeWPPh <sub>2</sub> Et	3a	110 (1)	18 (1)	-27 (1)	137	115	-34	4
trans-Cp(OC) <sub>2</sub> MeWPPh <sub>2</sub> Pr	3b	118 (1)	7 (2)	-33 (2)	151	131	-47	4
trans-Cp(OC) <sub>2</sub> MeWPPh <sub>2</sub> Bu	3c	116 (2)	6 (10)	-38 (11)	154	132	-43	3
		120 (3)	-9 (7)	-35 (9)	155	142	-66	3
trans-Cp(OC) <sub>2</sub> MeWPPh <sub>2</sub> Pe	3d	117 (1)	5 (4)	-37 (3)	154	133	-58	4
(OC) <sub>4</sub> MnPPh <sub>2</sub> (CH <sub>2</sub> ) <sub>3</sub>	4b	181	92	-21	202	146	12	1
(OC) <sub>4</sub> MnPPh <sub>2</sub> (CH <sub>2</sub> ) <sub>4</sub>	4c	121 (2)	38 (1)	-34 (2)	155	119	-7	2
Cp(OC) <sub>2</sub> WPPh <sub>2</sub> (CH <sub>2</sub> ) <sub>3</sub>	5b	169 (1)	99 (1)	-46 (1)	215	143	35	4
Cp(OC) <sub>2</sub> WPPh <sub>2</sub> (CH <sub>2</sub> ) <sub>4</sub>	5c	114 (2)	-15 (1)	-49 (2)	163	146	-58	4
Cp(OC) <sub>2</sub> MoPPh <sub>2</sub> (CH <sub>2</sub> ) <sub>3</sub>	6b	209 (1)	143 (1)	-50 (1)	259	163	49	4
Cp(OC) <sub>2</sub> MoPPh <sub>2</sub> (CH <sub>2</sub> ) <sub>4</sub>	6c	154 (1)	34 (1)	-34 (2)	188	154	-28	4
(OC) <sub>4</sub> MnPPh <sub>2</sub> (CH <sub>2</sub> ) <sub>2</sub> SO <sub>2</sub>	7b	156 (3)	78 (4)	-17 (7)	173	126	10	2
(OC) <sub>4</sub> MnPPh <sub>2</sub> (CH <sub>2</sub> ) <sub>3</sub> SO <sub>2</sub>	7c	85 (1)	23 (2)	-35 (1)	120	91	-3	2
(OC) <sub>4</sub> MnPPh <sub>2</sub> (CH <sub>2</sub> ) <sub>4</sub> SO <sub>2</sub>	7d	99 (1)	58 (2)	-6 (2)	105	73	22	2

<sup>a</sup> From graphical analysis of sideband intensities<sup>10</sup> or from singularities of the powder pattern; standard deviations in parentheses. <sup>b</sup> For abbreviations see Table I. <sup>c</sup> Anisotropy range  $\mu = \delta_{33} - \delta_{11}$ . <sup>d</sup> Anisotropy parameter  $\Delta\delta = \delta_{11} - (\delta_{22} + \delta_{33})/2$ . <sup>e</sup> Asymmetry parameter  $\rho = (\delta_{11} + \delta_{33} - 2\delta_{22})/(\delta_{33} - \delta_{11})$ .<sup>10</sup>

To separate the effects on the phosphorus-31 shielding by ring closure from other influences, we studied the acyclic compounds 1–3. The manganese complexes 1 differ by up to 15 ppm in their respective tensor components (Table II, Figure 2) due to changes in the bond angles at phosphorus and variations of the torsional angle Br–Mn–P–C(alkyl). The structural differences in bond and torsional angles were obtained from single-crystal X-ray diffraction studies of 1b–d;<sup>7,13</sup> i.e., the bond angles Mn–P–C(alkyl) have the values 112.4 (1b), 118.4 (1c), and 117.8° (1d) and the torsional angles Br–Mn–P–C(alkyl) the values -48 (1b), -19 (1c), and -28° (1d).

When comparing the principal elements of the piano stool complex 2c with those of compound 3c (Table II), one must account for the fact that 2c and 3c have cis and trans geometries, respectively, and in 3c the chlorine of 2c is substituted by a methyl group. In general, the difference in the chemical shifts in solution between cis and trans geometries in comparable piano stool compounds is small (3–6 ppm).<sup>14,15</sup> In the case of 2c and 3c the trans influence<sup>16–18</sup> of a ligand effects a large change in only one of the tensor components. While the respective tensor components  $\delta_{22}$  and  $\delta_{33}$  of compounds 2c and 3c are almost constant (Figure 2),  $\delta_{11}$  is shifted 60–70 ppm downfield in 3c. This may be caused mainly by the different bond-weakening abilities of the chlorine and the methyl group.

In solution, the isotropic tumbling of molecules compensates effects due to the electronic and steric structure of the molecule. This may result in similar isotropic chemical shifts in such quite different complexes as 2c (13.3 ppm) and 5c (16.4 ppm). The distinct character of 2c and 5c is better described by the chemical shift anisotropy, which may be expressed by the anisotropy range:  $\mu(2c) = 79.3$ ,  $\mu(5c) = 162.7$  ppm.

Compound 3c exhibits two different signals separated by 3 ppm in the solid-state  $^{31}\text{P}$  NMR spectrum in a 1:1 ratio, which indicate two distinct species (Figure 2). The CP/MAS spectrum and the

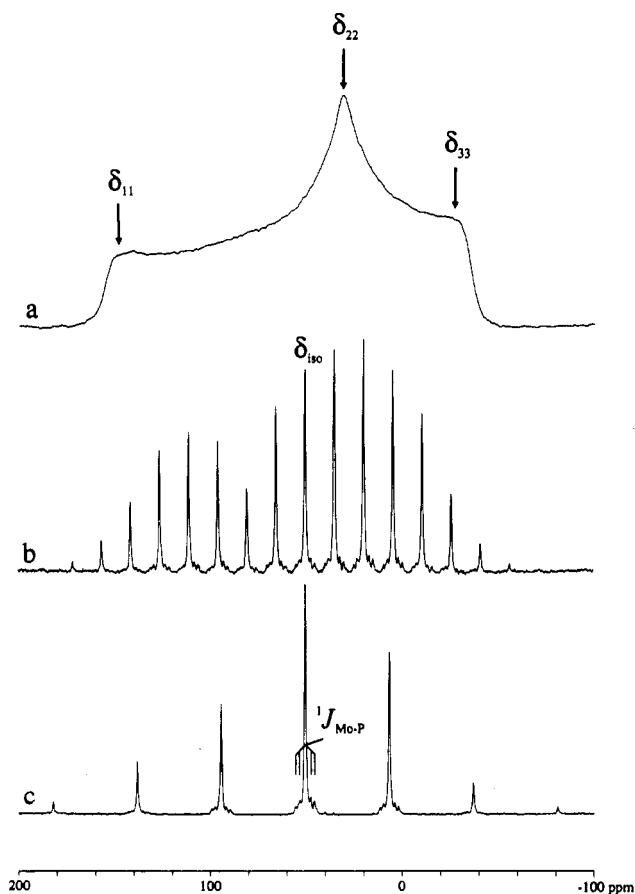


**Figure 1.**  $^{31}\text{P}$  CP solid-state NMR spectra of  $\text{Cp}(\text{OC})_2\text{MoPPh}_2(\text{CH}_2)_4$  (6c) obtained at 81.000 MHz with proton dipolar decoupling: (a) stationary sample with principal elements of the chemical shift tensor (512 scans); (b) sample spinning at the magic angle (rotor frequency = 1232 Hz, 256 scans); (c) sample as in part b with rotor frequency = 3548 Hz.

powder pattern show that only  $\delta_{22}$  of the two species differs. This phenomenon of inequivalent species in the solid state is often observed and is normally attributed to nuclei in positions not related by symmetry.<sup>19</sup>

- (13) Fawzi, R. Unpublished results.  
 (14) George, T. A.; Sterner, C. D. *Inorg. Chem.* **1976**, *15*, 165.  
 (15) Lindner, E.; Stangle, M.; Hiller, W.; Fawzi, R. *Chem. Ber.* **1988**, *121*, 1421.  
 (16) (a) Gambaro, J. J.; Hohman, W. H.; Meek, D. W. *Inorg. Chem.* **1989**, *28*, 4154. (b) Pidcock, A.; Richards, R. E.; Venanzi, L. M. *J. Chem. Soc. A* **1966**, 1707.  
 (17) George, T. A.; Turnipseed, C. D. *Inorg. Chem.* **1973**, *12*, 394.  
 (18) Zumdahl, S. S.; Drago, R. S. *J. Am. Chem. Soc.* **1968**, *90*, 6669.

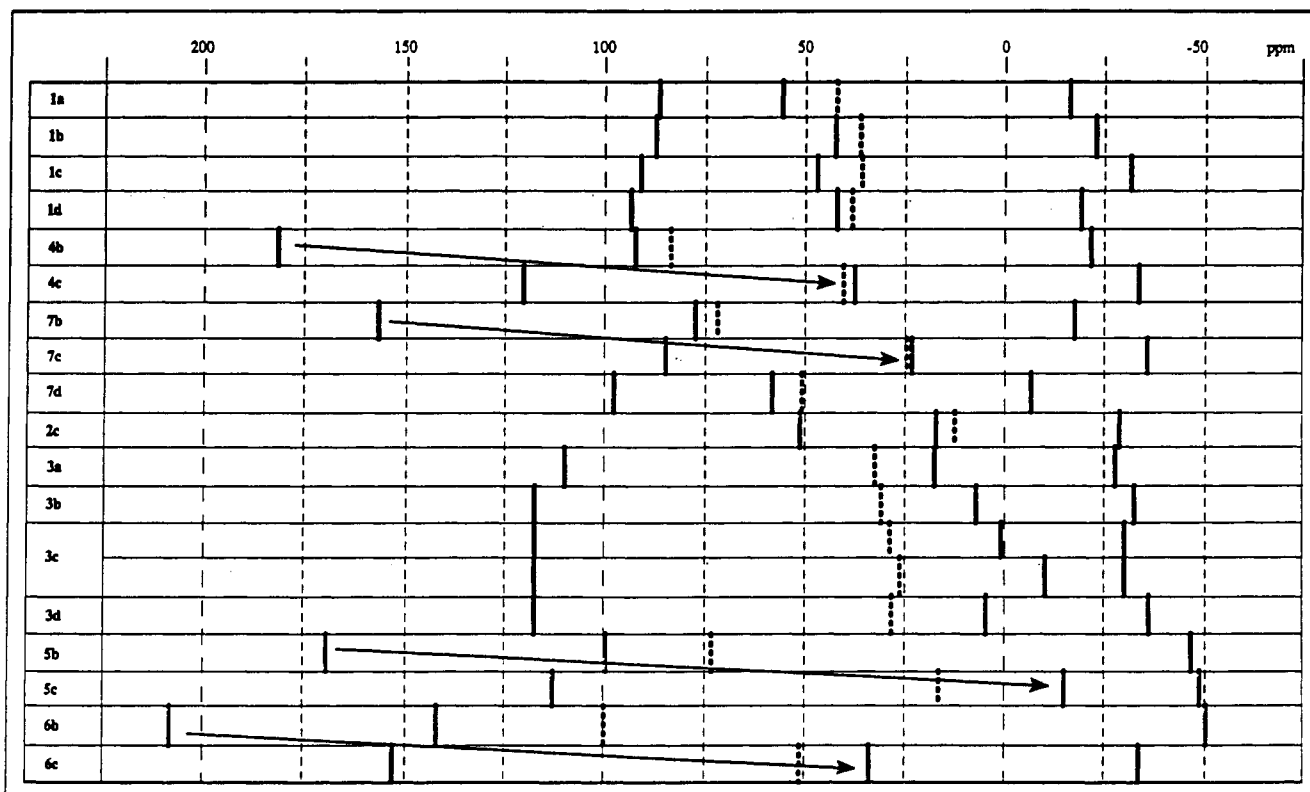


**Figure 2.** Observed stick spectra of <sup>31</sup>P NMR isotropic chemical shifts (dashed sticks) and tensor principal components (full sticks) of compounds 1–7, showing the crossover of  $\delta_{11}$  and  $\delta_{22}$  in the five- and six-membered cycles.

The shielding tensor component  $\delta_{33}$  shows no systematic changes with variation of the geometry or of the substituents within compounds 1–7. There is a dependence upon the choice of the metal. This is demonstrated by the manganese complexes 1, 4, and 7 with  $\delta_{33}$  values of  $-23 \pm 9$  ppm and the tungsten complexes 2, 3, and 5 with  $\delta_{33}$  values of  $-37 \pm 7$  ppm (Figure 2), but one must account for the fact that these ranges do overlap and changes within one class of compounds may be larger than the difference between these ranges. Upon a change in the ring size, the center shielding tensor component of the six-membered rings 4c–7c experiences a strong downfield shift (130–240 ppm) and thus becomes the low-field component of the chemical shift tensor in the five-membered rings 4b–7b. This crossover of  $\delta_{22}$  and  $\delta_{11}$  is also observed for the carbon-13 shielding components in the series cyclopropane/cyclobutane/cyclopentane and is interpreted in terms of changes in bond angles.<sup>20</sup> The exceptional behavior of the five-membered rings is also expressed in their positive asymmetry parameters  $\rho$  (Table II), whereas in the cases of 4c–7c and 3 this parameter is negative.

The chemical shift anisotropy pattern of a powdered sample yields only the magnitudes of the shielding, not the directional elements.<sup>8</sup> A single-crystal <sup>31</sup>P NMR study carried out for the Wilkinson catalyst ClRh(PPh<sub>3</sub>)<sub>3</sub> shows that  $\delta_{33}$  of all three phosphines is directed toward the metal atom.<sup>21</sup> In 5 and 6  $\delta_{33}$ , which we also assume to be directed toward the metal, varies slightly (Figure 2). However, upon comparison of the tensor components  $\delta_{11}$  and  $\delta_{22}$ , which are perpendicular to the metal–phosphorus bond, a downfield shift of  $43 \pm 4$  ppm is observed when tungsten is replaced by molybdenum. This is in accord with theoretical predictions for the directionality of the heavy-atom shift.<sup>22–25</sup>

The one-bond <sup>31</sup>P–M (M = <sup>55</sup>Mn,  $I = 5/2$ , 100%; M = <sup>95</sup>Mo,  $I = 5/2$ , 15.7%; M = <sup>97</sup>Mo,  $I = 5/2$ , 9.5%; M = <sup>183</sup>W,  $I = 1/2$ , 14.4%) coupling constants contain additional structural information.<sup>1</sup> Because the <sup>1</sup>J<sub>W–P</sub> coupling constants in the <sup>31</sup>P CP/MAS NMR spectra are of the order of the line width, they are not always resolved. In spite of this, it is possible to extract the coupling constants by computational simulation of the line shape (Table I). With the exception of those of 5b, which adopts different conformations in solution and in the solid state,<sup>7</sup> the calculated coupling constants are in good agreement with the values obtained in solution. The coupling between <sup>31</sup>P and <sup>95/97</sup>Mo is normally not detectable with solution <sup>31</sup>P NMR spectroscopy, although values known from solution <sup>95</sup>Mo NMR spectroscopy are in the range 130–220 Hz.<sup>26</sup> However, the <sup>31</sup>P CP/MAS NMR spectra of 6b,c display satellites due to coupling of <sup>31</sup>P to <sup>95/97</sup>Mo (Figure 1c). The metal–phosphorus interactions <sup>183</sup>W–<sup>31</sup>P and <sup>95/97</sup>Mo–<sup>31</sup>P show the same trend, both being larger in the five-membered cycles 5b and 6b than in the six-membered rings 5c and 6c. The ratio <sup>1</sup>J<sub>W–P</sub>:<sup>1</sup>J<sub>Mo–P</sub> is (1.5–1.8):1, as stated elsewhere.<sup>26</sup>

Nuclei with spin  $I > 1/2$  are quadrupolar due to a nonspherical charge distribution.<sup>27</sup> In the case of manganese, for example, this results in a distortion of the solid-state NMR spectra, which depends on the relative magnitudes of the quadrupole coupling constant  $\chi = eQV_{zz}/h$  and the Larmor frequency  $Z_{Mn}$  of manganese.<sup>28</sup> The perturbations brought about by this interaction are transmitted via dipolar coupling to the neighboring phosphorus nucleus, producing first-order ( $\chi$  small, Figure 3a) or second-order perturbations ( $\chi$  large, Figure 3b). In these cases, the effective tensor has principal elements that depend on both the chemical shielding anisotropy and the quadrupole interaction,<sup>11,29</sup> and the

(19) Clayden, N. J. *Chem. Scr.* **1988**, *28*, 211.  
 (20) Facelli, J. C.; Grant, D. M. *Top. Stereochem.* **1989**, *19*, 1.  
 (21) Naito, A.; Sastry, D. L.; McDowell, C. A. *Chem. Phys. Lett.* **1985**, *115*, 19.  
 (22) Santos, R. A.; Chien, W.-J.; Harbison, G. S.; McCurry, J. D.; Roberts, J. E. *J. Magn. Reson.* **1989**, *84*, 357.  
 (23) Pyykkö, P.; Görling, A.; Rösch, N. *Mol. Phys.* **1987**, *61*, 195.  
 (24) Nomura, Y.; Takeuchi, Y. *Tetrahedron Lett.* **1969**, *8*, 639.  
 (25) Pyykkö, P. *Chem. Rev.* **1988**, *88*, 563.

(26) Masters, A. F.; Bossard, G. E.; George, T. A.; Brownlee, R. T. C.; O'Connor, M. J.; Wedd, A. G. *Inorg. Chem.* **1983**, *22*, 908.  
 (27) Kidd, R. G.; Goodfellow, R. J. In *NMR and the Periodic Table*; Harris, R. K., Mann, B. E., Eds.; Academic Press: London, 1978.  
 (28) (a) Smith, J. A. S. *Chem. Soc. Rev.* **1986**, *15*, 225. (b) Cohen, M. H.; Reif, F. In *Solid State Physics*; Seitz, F., Turnbull, D., Eds.; Academic Press: New York, 1957; Vol. 5.  
 (29) Power, W. P.; Wasylishen, R. E.; Mooibroek, S.; Pettitt, B. A.; Danchura, W. J. *Phys. Chem.* **1990**, *94*, 591.

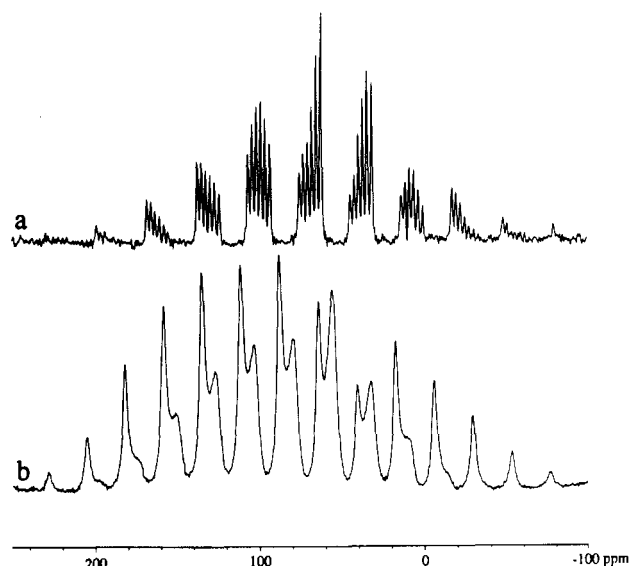


**Figure 3.** Solid-state  $^{31}\text{P}$  CP/MAS NMR spectra obtained at 81.000 MHz: (a)  $(\text{OC})_4\text{MnPPH}_2(\text{CH}_2)_2\text{SO}_2$  (**7b**), showing first-order quadrupolar effects (rotor frequency = 2500 Hz, 256 scans); (b)  $(\text{OC})_4\text{MnPPH}_2(\text{CH}_2)_3$  (**4b**), showing second-order quadrupolar effects (rotor frequency = 1594 Hz, 512 scans).

line shape of the spinning sidebands need not necessarily be the same as the center band (Figure 3b).<sup>30</sup> The different intensities of the transitions within the multiplets (Figure 3a) are caused by the Mn–P dipolar interaction.

In the  $^{31}\text{P}$  CP/MAS spectra of **1** and **7** the scalar coupling of  $^{55}\text{Mn}$  and  $^{31}\text{P}$  is well resolved, resulting in a multiplet of six lines which are not equidistant due to the dipolar interaction of the quadrupole with the spin  $1/2$  nucleus (Figures 3a and 4a).<sup>31–33</sup> Application of first-order perturbation treatment according to Olivieri<sup>34</sup> allows us to extract the scalar coupling constant  $J_{\text{iso}}$  (Table I) and a value  $d$  which is characteristic for the distortion of the multiplet (Figure 4a):

$$d = -(3\chi D / 20Z_{\text{Mn}})(3 \cos^2 \beta^D - 1 + \eta \sin^2 \beta^D \cos 2\alpha^D) \quad (1)$$

where  $\eta = (V_{XX} - V_{YY})/V_{ZZ}$  is the asymmetry parameter of the EFG tensor,  $Z_{\text{Mn}}$  is the Zeeman frequency of  $^{55}\text{Mn}$  in the applied field,  $D = (\mu_0/4\pi)(\gamma_{\text{P}}\gamma_{\text{Mn}}/r_{\text{Mn-P}}^3)(\hbar/4\pi^2)$  is the dipolar coupling constant, and  $\beta$  and  $\alpha$  are polar and azimuthal angles that define the orientation of the internuclear vector in the principal-axis system of the EFG at  $^{55}\text{Mn}$ .<sup>34</sup> The observed values of  $J_{\text{iso}}$  are in the usual range of  $^1J_{\text{Mn-P}}$  coupling constants<sup>35</sup> and do not change significantly between compounds **1** and **7**.

If some assumptions are made, the experimental value of  $d$  can be compared with that predicted by eq 1, as will be demonstrated for compound **1d** as an example. With the known Mn–P distance of 235.8 pm,<sup>7</sup> the direct dipolar coupling constant is calculated to be  $D = 915$  Hz. Values of the quadrupole coupling constant  $\chi$  and the asymmetry  $\eta$  are obtained by application of a model calculation.<sup>36</sup> With the expressions for an octahedral *cis*-MB<sub>4</sub>AC species<sup>36</sup> (see also Figure 4c) and the partial quadrupole splitting values (pqs) for the ligands  $-0.28$  (Br),  $-0.55$  (CO),<sup>37</sup>  $-0.53$  mm

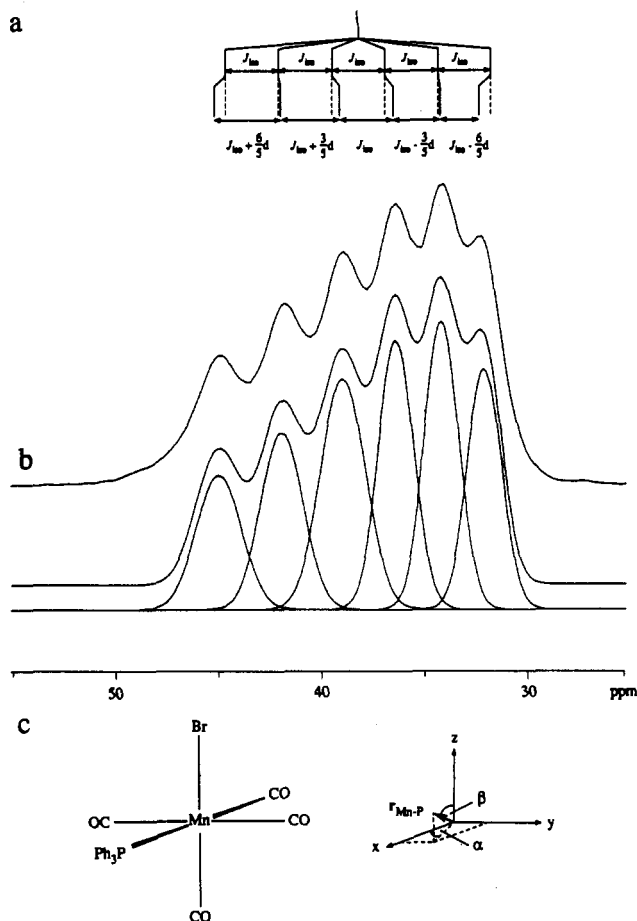


**Figure 4.** Center peak in the  $^{31}\text{P}$  CP/MAS NMR spectrum of  $(\text{OC})_4\text{BrMnPPH}_2\text{Pe}$  (**1d**) (rotor frequency = 3600 Hz, 112 scans): (a) schematic representation of the spectrum of phosphorus affected by the quadrupolar nucleus  $^{55}\text{Mn}$ ; (b) experimental spectrum (upper trace) and simulated line shape (bottom); (c) angles  $\alpha$  and  $\beta$  defining the orientation of the Mn–P bond in the electric field gradient tensor at manganese.<sup>36</sup>

**Table III.** Calculated Values of  $d$  (Eq 1) for Different Orientations of  $r_{\text{Mn-P}}$  (Cf. Figure 4c) in the EFG Tensor at Manganese ( $\chi = 16.9$  MHz,  $D = 915$  Hz,  $Z_{\text{Mn}} = 49.328$  MHz)

$\beta^D$ , deg	0	0	90	90 <sup>a</sup>	90	90	90
$\alpha^D$ , deg	0	0	0	0 <sup>a</sup>	0	90	90
$\eta$	0	1	0	0.12 <sup>a</sup>	1	0	1
$d$	-94	-94	+47	+41	0	-47	-94

<sup>a</sup> Values obtained from the point-charge model.<sup>36</sup>

$s^{-1}$  (PPh<sub>3</sub>),<sup>38</sup> we are able to calculate the electric field gradients  $V_{ii}$  and the asymmetry parameter  $\eta$  for  $^{55}\text{Mn}$  using  $1 \text{ mm s}^{-1} = 32.4 \text{ MHz}$ .<sup>39</sup> Thus,  $\eta$  and  $\beta^D$  are estimated to be 0.12 and 90°, respectively, and the quadrupolar coupling constant  $\chi$  is calculated to be 16.9 MHz, which is in the range of  $\chi$  for  $\text{BrMn}(\text{CO})_5$  (17.5 MHz).<sup>38</sup>

Equation 1 indicates that  $d$  depends on both the sign and the magnitude of  $\chi$  and on the orientation of the Mn–P bond relative to the principal-axis system of the EFG tensor at manganese. To show this dependence, we have calculated values of  $d$  for different orientations of this internuclear vector (Table III). The value obtained from our simple model is in good agreement with experiment (Table I).

In the  $^{31}\text{P}$  CP/MAS spectra of compounds **7**,  $d$  has a sign opposite to that of  $d$  in series **1**. The line shape of the center peak in the  $^{31}\text{P}$  CP/MAS spectrum of compound **4b** (Figure 3b) is

- (30) Zumbulyadis, N.; Henrichs, P. M.; Young, R. H. *J. Chem. Phys.* **1981**, *75*, 1603.  
 (31) Hexem, J. G.; Frey, M. H.; Opella, S. J. *J. Chem. Phys.* **1982**, *77*, 3847.  
 (32) Apperley, D. C.; Haiping, B.; Harris, R. K. *Mol. Phys.* **1989**, *68*, 1277.  
 (33) (a) Menger, E. M.; Veeman, W. S. *J. Magn. Reson.* **1982**, *46*, 257. (b) Bowmaker, G. A.; Cotton, J. D.; Healy, P. C.; Kildea, J. D.; Silong, S. B.; Skelton, B. W.; White, A. H. *Inorg. Chem.* **1989**, *28*, 1462.  
 (34) (a) Olivieri, A. C. *J. Magn. Reson.* **1989**, *81*, 201. (b) Olivieri, A. C.; Frydman, L.; Diaz, L. E. *J. Magn. Reson.* **1987**, *75*, 50.  
 (35) Rehder, D.; Bechthold, H.-C.; Kececi, A.; Schmidt, H.; Siewing, M. *Z. Naturforsch.* **1982**, *37B*, 631.  
 (36) Bancroft, G. M.; Platt, R. H. *Adv. Inorg. Chem. Radiochem.* **1972**, *15*, 59.  
 (37) Bancroft, G. M.; Butler, K. D.; Libbey, E. T. *J. Chem. Soc., Dalton Trans.* **1972**, 2643.

- (38) Ireland, P. S.; Deckert, C. A.; Brown, T. L. *J. Magn. Reson.* **1976**, *23*, 485.  
 (39) Bancroft, G. M.; Clark, H. C.; Kidd, R. G.; Rake, A. T.; Spinney, H. *G. Inorg. Chem.* **1973**, *12*, 728.

typical for second-order quadrupolar effects,<sup>40</sup> indicating a large quadrupolar coupling constant. Signs and magnitudes of  $\chi$  change with the  $\sigma$ -donor/ $\pi$ -acceptor strength of the ligands,<sup>27,39</sup> in agreement with the order  $\text{Br} < \text{SO}_2\text{R} < \text{CH}_2\text{R}$  in compounds 1, 7, and 4.

### Conclusions

The use of phosphorus-31 chemical shift tensors as accessible NMR parameters and their correlation to structure is only beginning.<sup>41-43</sup> In the present paper we have been able to demonstrate the amplified sensitivity of the different shielding components affected by the local environment of the nuclei. Examples are the different trans influences of the chlorine and the methyl

group, which cause a change of 70 ppm in  $\delta_{11}$  only. Also, the known dependence of the phosphorus chemical shift on the ring size in chelate systems was found to be due to a single tensor component.

We have also shown that it is possible to observe <sup>55</sup>Mn- and <sup>95/97</sup>Mo-<sup>31</sup>P coupling constants in the <sup>31</sup>P CP/MAS spectra, which are not accessible in solution because of fast relaxation processes. In the case of the manganese complex 1d, the solid-state <sup>31</sup>P NMR spectrum has provided the opportunity to obtain the sign and magnitude of the manganese quadrupolar coupling constant and the asymmetry parameter, parameters not easily obtainable with other methods.<sup>36</sup> The knowledge of such quadrupolar interactions helps achieve a deeper insight into the nature of bonding in such complexes. Further investigations are in progress.

**Acknowledgment.** Support of this work by the Deutsche Forschungsgemeinschaft, Bonn/Bad Godesberg, by the Fonds der Chemischen Industrie, Frankfurt/Main, by BASF Aktiengesellschaft, and by Schering AG is gratefully acknowledged. Thanks are also due to C. Kingston for reading the manuscript.

- (40) Ganapathy, S.; Schramm, S.; Oldfield, E. *J. Chem. Phys.* **1982**, *77*, 4360.  
 (41) Carty, A. J.; Fyfe, C. A.; Lettinga, M.; Johnson, S.; Randall, L. H. *Inorg. Chem.* **1989**, *28*, 4120.  
 (42) Penner, G. H.; Wasylshen, R. E. *Can. J. Chem.* **1989**, *67*, 1909.  
 (43) Tullius, M.; Lathrop, D.; Eckert, H. *J. Phys. Chem.* **1990**, *94*, 2145.

Contribution from the Departments of Chemistry, Indiana University, Bloomington, Indiana 47405, and University of Vermont, Burlington, Vermont 05405

## The Transient Radical $\text{H}_3\text{Ir}(\text{PMe}_2\text{Ph})_3^+$ : A Bronsted Acid

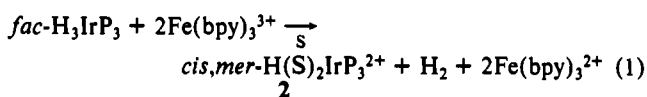
D. Eric Westerberg, Larry F. Rhodes, Joseph Edwin, William E. Geiger, and Kenneth G. Caulton\*

Received September 18, 1990

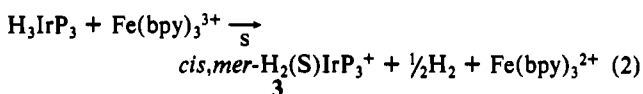
Electrochemical oxidation ( $E_p = +0.55\text{V}$  vs SCE) or one-electron outer-sphere oxidation of  $\text{fac-H}_3\text{IrP}_3$  ( $\text{P} = \text{PMe}_2\text{Ph}$ ) by either  $\text{Fe}(\text{bpy})_3^{3+}$  or  $\text{Cp}_2\text{Fe}^+$  yields  $\text{H}_2\text{Ir}(\text{S})\text{P}_3^+$ ,  $\text{S} = \text{MeCN}$  or acetone. In  $\text{CH}_2\text{Cl}_2$ ,  $\text{H}_4\text{IrP}_3^+$  is a detectable product. It is concluded that these are the stoichiometric (equimolar) primary products of reaction of the transient radical  $[\text{H}_3\text{IrP}_3^{\bullet}]$  with  $\text{fac-H}_3\text{IrP}_3$ . Scavenging with  $\text{NEt}_3$  or pyridine reveals that this reaction proceeds by proton transfer from  $\text{H}_3\text{IrP}_3^+$  and that this radical is not effectively quenched by the hydrogen atom donors <sup>1</sup>PrOH or cumene nor by the H atom acceptor  $[\text{CPh}_3]^+$ . It is proposed that the transient radical has the composition  $\text{Ir}(\text{H}_2)\text{HP}_3^+$ .

### Introduction

Recently, we suggested<sup>1</sup> the use of a strong outer-sphere oxidant,  $\text{Fe}(\text{bpy})_3(\text{PF}_6)_3$ , as a method for quantitating the number of metal-bound ligands  $\text{M-H}$  (as  $\text{H}_2$ ) or  $\text{M-CO}$  (as  $\text{CO}$ ) by Toepler pumping of the noncondensable gases evolved following oxidation. For the polyhydride  $\text{fac-H}_3\text{Ir}(\text{PMe}_2\text{Ph})_3$ , oxidation by 2 or more equiv of  $\text{Fe}(\text{bpy})_3(\text{PF}_6)_3$  resulted in the liberation of 1 mol of  $\text{H}_2/\text{Ir}$  (eq 1,  $\text{P} = \text{PMe}_2\text{Ph}$ ,  $\text{S} = \text{MeCN}$ ). This stoichiometry raises the



possibility of an intramolecular mechanism for elimination of  $\text{H}_2$  from some cationic iridium trihydride radical. Such a mechanism has been shown<sup>2</sup> to fold for  $\text{H}_2$  elimination from *diamagnetic*  $\text{H}_3\text{OsP}_3^+$ . However, further study of eq 1 revealed that 1 equiv of oxidant results in complete consumption of  $\text{H}_3\text{IrP}_3$  but the loss of only  $1/2$  mol of  $\text{H}_2/\text{Ir}$  (eq 2,  $\text{S} = \text{MeCN}$ ). This result is totally

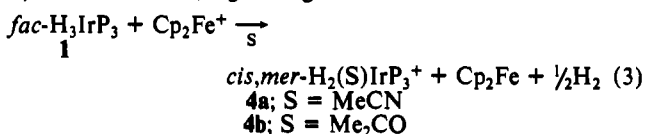


unexpected on the basis of an intramolecular  $\text{H}_2$  elimination mechanism and suggests instead that an intermolecular mechanism may be operative. Also relevant is the fact that paramagnetic polyhydrides devoid of  $\pi$ -donor ligands are unknown. The implied high reactivity of such species has been verified for the transient radical  $\text{ReH}_6(\text{PMe}_2\text{Ph})_2$ .<sup>3</sup> Even dimetal paramagnetic polyhydrides are highly reactive.<sup>4</sup> To gain a better understanding

of the results and mechanistic implications of eq 2, we have explored in more detail this oxidation and report our findings here.

### Results

**Oxidation in Coordinating Solvents.** In order to avoid the possibility of "overoxidation" of  $\text{fac-H}_3\text{IrP}_3$ <sup>5</sup> by  $\text{Fe}(\text{bpy})_3^{3+}$  (eq 1), the stoichiometry of eq 2 was studied by using the milder oxidant,  $\text{Cp}_2\text{FeBF}_4$  ( $E^\circ = +0.55\text{V}$  vs  $E^\circ = +1.21\text{V}$  for  $\text{Fe}(\text{bpy})_3^{3+}$  vs SCE). The potential of oxidation of  $\text{H}_3\text{IrP}_3$  (+0.55 V) is coincidentally the same as that of ferrocene in these media. In spite of this, ferrocenium is able to exhaustively oxidize the Ir complex because the irreversibility of the  $\text{H}_3\text{IrP}_3$  oxidation allows the reaction to proceed to completion. We have also employed two different solvents, acetonitrile and acetone. At low temperature, the reactions were complete in minutes with quantitative consumption of ferrocenium ion (as judged by the absence of its blue color) to yield the corresponding solvent cations (eq 3). In both cases, vigorous gas evolution was noted when the



reaction was carried out at room temperature. Thus, the ferro-

- (1) Lemmen, T. H.; Lundquist, E. G.; Rhodes, L. F.; Sutherland, B. R.; Westerberg, D. E.; Caulton, K. G. *Inorg. Chem.* **1986**, *25*, 3915.
- (2) Bruno, J. W.; Huffman, J. C.; Caulton, K. G. *J. Am. Chem. Soc.* **1984**, *106*, 1663.
- (3) Bruno, J. W.; Caulton, K. G. *J. Organomet. Chem.* **1986**, *315*, C13.
- (4) Allison, J. D.; Walton, R. A. *J. Am. Chem. Soc.* **1984**, *106*, 163.
- (5) We have chosen to study the oxidation reactions of the facial isomer (*vis-à-vis* the meridional isomer) only because of its ease of isolation and purification. The cyclic voltammogram of a mixture of *fac* and *mer* isomers is identical with that of pure *fac*, suggesting no dramatic difference in behavior for the *mer* isomer.

\* To whom correspondence should be addressed at Indiana University.